

Some properties of poly[bis(halophenoxy)phosphazenes]

M. Kojima, S. G. Young and J. H. Magill*

Department of Materials Science and Engineering, School of Engineering,
University of Pittsburgh, Pittsburgh, PA 15261, USA

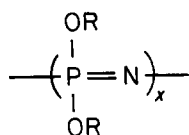
(Received 2 September 1991; revised 23 January 1992; accepted 18 February 1992)

The morphology and structure of poly[bis(halophenoxy)phosphazenes] (PBHPP) with F, Cl and Br substituents in the *para*- or *meta*-phenoxy positions have been investigated. The size and position of halogen atoms have a significant influence on the thermotropic transition of the polymer. Most PBHPP exhibit polymorphism. Monoclinic and orthorhombic three-dimensional crystalline forms and the location of the two-dimensional mesophase depend upon the chemistry and thermal history of each polymer specimen. Most of the physical properties may be related to the location of the thermotropic transition of the polyphosphazene, which can be expressed as a linear function of the substituent size. Polyphosphazene crystallization behaviour appears to depend upon the position and size of halogen atoms, and the growth of well defined crystals becomes difficult with enhanced side-group size. Surprisingly, thick or bulk specimens of PBHPP comprise globules of comparatively uniform size, which depend upon the sample preparation conditions and the kind of halogen atom present in the side-group. The dimensions of these globules may be increased by heat treatment and with an increase in crystallinity of each polymer specimen. The globules exhibit a bundle-like texture even in drawn PBHPP films.

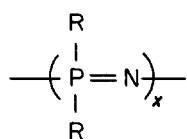
(Keywords: thermotropic transition; solution casting; polymorphism; X-ray diffraction; electron diffraction; density; morphology; fracture surface; globular texture; poly[bis(halophenoxy)phosphazenes])

INTRODUCTION

Recently, interest in thermotropic phosphazene homopolymers has focused on the influence of the side-group chemistry on thermotropic behaviour^{1,2}. Most semicrystalline poly(organophosphazenes), including copolymers³, with alkoxy or aryloxy substituents, exhibit a first-order thermotropic transition $T(1)$. The transition is found to be strongly influenced by the type, size, polarity and flexibility of the side-groups attached to the phosphorus atom. The structure of poly(organophosphazenes):



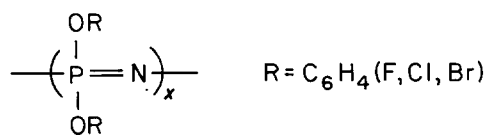
has been studied⁴⁻¹⁹, but detailed investigations are sparse. Polymorphic and so-called mesomorphic forms of phosphazene homopolymers with various side-groups have been reported^{8-13,16,18}. Other polyphosphazenes having alkyl and even aryl side-groups linked directly to the backbone phosphorus:



as in poly(dimethylphosphazene) also exhibit thermotropic behaviour^{20,21}. Until now, crystalline polyphosphazenes were reported only when the group

mesogen was attached to the phosphorus through a sufficiently flexible spacer unit such as oxygen, for example, which can facilitate disordered side-group conformations, which characterize the thermotropic state. Surprisingly, our recent work has shown that mesophase behaviour is also observed in the absence of a spacer, presumably because of the flexible chain backbone²¹. Whenever the 3D crystals of poly(organophosphazenes) transform into the 2D disordered phase, it has been established that the molecular chains adopt a pseudo-hexagonal arrangement, when considerable expansion occurs transverse to the molecular chain axis direction^{22,23}. A crystallographic axial relationship¹² between the 3D crystals and the 2D phase has been established and demonstrated for poly[bis(phenoxy)phosphazene] (PBPP)[†]. A linear relationship has been shown to exist between the intermolecular chain separation in the thermotropic phase and the side-group dimensions of selected polyphosphazenes^{1,2}.

Furthermore, a linear empirical relationship connecting the glass transition temperature T_g , the melting temperature T_m and the thermotropic transition temperature $T(1)$ has been established for many semicrystalline poly(organophosphazenes)². Aspects of poly[bis(halophenoxy)phosphazenes]:



*To whom correspondence should be addressed. Present address: ONR Europe, 223-231 Old Marylebone Road, London NW1 5TH, UK

†This terminology is used in line with literature usage instead of the more correct nomenclature PDPP signifying the diphenoxy side-groups

have been reported in the literature^{2-4,16,22,24,25}. In the chemical formula the phenoxy group is halogenated in the *meta* or *para* position. Synthesis and characterization and dynamic mechanical measurements and tensile tests of PB(4-Cl)PP have been reported²². X-ray diffraction measurements for PB(4-Cl)PP and PB(3-Cl)PP in the thermotropic phase have been made²⁴, and it has been found that the transformation involves an expansion from the 3D orthorhombic phase to the 2D mesophase with a considerable change in unit-cell dimensions, e.g. about 9% in the *a* axis and 20% in the *b* axis direction, respectively, for PB(4-Cl)PP²⁴. Crystals of PB(4-F)PP grown from xylene solution are monoclinic. When specimens are heated above $T(1)$ and then cooled to room temperature, the crystal transforms from the monoclinic via a 2D hexagonal phase into the orthorhombic state. Twinning occurs frequently during this phase change from the 2D thermotropic phase to the 3D orthorhombic form¹⁶ for PB(HP)P specimens and for poly[bis(trifluoroethoxy)phosphazene]⁸. Here the notation (HP) in the abbreviation means halogenated phenoxy group. Studies of the morphological and structural features associated with the $T(1)$ behaviour in PBHPP are still in progress. This paper reports on interesting aspects of morphology, structure and thermotropic properties of these polymers.

EXPERIMENTAL

Materials

Poly[bis(halophenoxy)phosphazenes] have been made by reacting poly(dichlorophosphazene) with sodium *p*- or *m*-halophenoxide in solution in tetrahydrofuran (THF). The polymers synthesized²⁶ for this paper are

Table 1 G.p.c. analysis results for PBHPP used in this study

Polymer	M_n ($\times 10^5$)	M_w ($\times 10^5$)	M_w/M_n
PB(4-F)PP	6.6	25.8	3.9
PB(4-Cl)PP	4.4	17.9	4.1
PB(4-Br)PP	4.3	15.5	3.6
PB(3-F)PP	4.6	14.4	3.2
PB(3-Cl)PP	3.7	8.9	2.4
PB(3-Br)PP	6.6	23.3	3.5

Table 2 Some elemental analysis of PBHPP-type polyphosphazenes^a

Substituent halogen	C	N	P	F	Cl	Br	H	O	
4-Cl	48.5	4.4	10.3	—	22.7	—	—	—	Found
	48.0	4.7	10.3	0	23.6	0	2.7	10.7	Calcd
4-Br	37.0	3.5	7.7	—	—	40.7	—	—	Found
	37.1	3.6	8.0	0	0	41.1	2.1	8.2	Calcd
3-Cl	48.2	5.1	—	—	—	—	2.6	—	Found
	48.0	4.7	10.3	0	23.6	0	2.7	10.7	Calcd
3-Br	38.9	3.9	—	—	—	—	2.3	—	Found
	37.1	3.6	8.0	0	0	41.1	2.1	8.2	Calcd
4-F	54.2	—	10.5	—	—	—	2.8	12.5	Found
	54.0	5.2	11.6	14.2	0	0	3.0	12.0	Calcd

^aAll of the above showed no branching for ³¹P solution n.m.r. The i.r. spectra were normal too

listed in *Table 1*; molecular-weight characterization was made by g.p.c.

Fourier-transform infra-red (FTi.r.) spectra were obtained from 1600 to 400 cm^{-1} for each polymer sample synthesized. No P–O–P stretching or bending vibrations were present, indicating that, indeed, the desired linear polymer had been made. ³¹P and ¹³C solution n.m.r. analysis was also carried out, and these measurements were consistent with a linear polymer with the desired side-group chemistry. No P–OH groups were detected, which was evident from the characteristic peaks between the 2550–2700 and 2100–2300 cm^{-1} regions. For characterization purposes, elemental analyses were also made (see *Table 2*) to provide additional information about the materials investigated in this paper. More details are provided in an article to be published in *Polymer*²⁷.

Solution-grown crystals

Crystals of PB(4-F)PP were precipitated isothermally from a 0.001% w/w solution of polymer in *p*-xylene at 108°C¹⁶. Well defined crystals of the PBHPP type are more difficult to prepare as the size of the halogen atoms (hence the complexity of the side-group) increases.

Films

Polymer films of PBHPP examined by X-ray diffraction were prepared from THF solution (e.g. conc. 5% w/w) at 25°C. The films were often stretched at least 3–5 times at 25°C, or more below the $T(1)$ of each polymer. Such films used for transmission electron microscopy were prepared initially from 0.001% w/w solution of polymer in *p*-xylene, which was cast onto glycerol or phosphoric acid at temperatures below the respective $T(1)$ transitions of the PB(4-H)PP polymers (as e.g. at 135°C). The films so formed were washed several times with distilled water at room temperature to remove the adhering glycerol or phosphoric acid. The thicker films prepared for fracture surface examination by scanning electron microscopy and others for X-ray diffraction measurements were made from the polymer dissolved in THF. Fractured thick specimens were sometimes heated at 200°C (30 min) and then cooled to 25°C for examination of the orthorhombic phase.

Differential scanning calorimetry

A Perkin-Elmer DSC-2 calorimeter with an IBM PC computer was used for data acquisition and analysis through T_g , $T(1)$ and beyond²⁸.

X-ray diffraction measurements

X-ray diffraction measurements were made using a Statton-type vacuum camera fitted with heater and temperature controller within $\pm 1^\circ\text{C}$. Ni-filtered Cu K α radiation was used at 35 kV.

Electron microscopy

Transmission mode. Solution-grown crystals and thin cast films were examined mostly at 200 kV with a JEOL JEM-200 CX electron microscope. Specimens were often shadowed with Pd/Au (40/60) alloy.

Scanning mode. The fracture surface morphology was observed at 15 kV with a JEOL JSM-300 T and also with a Hitachi S-800 scanning microscope. Fracture surfaces were coated with Pd/Au (40/60) alloy or just Au itself.

Density measurements

The density of unheated and heat-treated cast films was measured at 25°C using a well known flotation method in aqueous CsCl solution. Density of PBHPP was also determined from dilatometry measurements made usually between room temperature and 200°C for carefully prepared clear discs of polymers using a vacuum press.

Solution n.m.r.

³¹P solution n.m.r. analysis was carried out with a Bruker 300 spectrometer to establish the chain linearity (non-branching nature) of the polyphosphazene used in this work.

RESULTS AND DISCUSSION

Thermotropic behaviour

D.s.c. measurements were carried out in the temperature range from about -60 to 200°C , which interval spanned the glass transition T_g and the thermotropic transition $T(1)$ temperatures of these halophenoxyphosphazenes. The thermal results are summarized in Table 3. After specimens were cooled from 200°C to room temperature at a rate of $10^\circ\text{C min}^{-1}$, then reheated in the d.s.c., a shift in the $T(1)$ peak position to higher temperature was always encountered under these circumstances. Besides, the enthalpy change $\Delta H_{T(1)}$ at $T(1)$ always increased significantly, reaching a value that is often double that of the original (unheated) specimens. However, PB(3-Br)PP appears to be the only exception to this behaviour, which may be associated with the crystallization ability of PB(3-Br)PP, which occurs markedly slower than for the other specimens. The trend in thermal behaviour reported with respect to $T(1)$ is common to all thermotropic phosphazene polymers²⁸. Generally, recycling specimens through the $T(1)$ transition increases notably the polymer crystallinity except for PB(3-Br)PP, which may be crystallized only very slowly from the 2D pseudohexagonal phase to the 3D stage. The $T(1)$ temperature increase is in line with the sizes and the change in polarity of the halogen substituents on going from F to Br on the phenyl mesogen in accordance with their smectic nature^{11,32}. For example, the physical parameters of PB(4-H)PP and PB(3-H)PP specimens fit the relationship:

$$3.2T_m^2 - [T_g + 8.2T(1)]T_m + 6T^2(1) = 0$$

which has already been established for other orthorhombic polyphosphazenes^{2,8,29}. Figure 1 shows the transition temperatures T_g , $T(1)$ and T_m (calculated using the above equation) for PBHPP polymers. Estimates are based on the atomic radii of the side-group atoms. The temperature range of the conformational disorder, $[T_m - T(1)]$, is the designated thermotropic span, which tends to correlate with the mobility and packing of the side-group

Table 3 Results of d.s.c. measurements for THF cast PBHPP films

Polymer	Polymer history ^a	T_g ($^\circ\text{C}$)	ΔC_p ($\text{cal g}^{-1} \text{K}^{-1}$)	$T(1)$ ($^\circ\text{C}$)	$\Delta H_{T(1)}$ (cal g^{-1})	T_c ($^\circ\text{C}$)	T_m^b ($^\circ\text{C}$)
PB(4-F)PP	I	-2	0.063	134	3.1	103	370
	II			146	6.9	105	
PB(4-Cl)PP	I	4	0.023	150	3.7	139	390
	II			171	7.1	141	
PB(4-Br)PP	I	24	0.076	156	2.0	131	420
	II			164	4.7	132	
PB(3-F)PP	I	-38	0.080	48	2.1	20	260
	II			49	4.0	21	
PB(3-Cl)PP	I	-24	0.074	66	2.5	35	290
	II			74	3.3	36	
PB(3-Br)PP	I	-15	0.044	81	3.7	35	320
	II			78	2.9	36	

^a(I) As cast

(II) Second run after being heated to 200°C and cooled to room temperature at $10^\circ\text{C min}^{-1}$

^bCalculated from the empirical equation²: $3.2T_m^2 - [T_g + 8.2T(1)]T_m + 6T^2(1) = 0$

substituents, the motion of which decreases with increasing side-group size. (Alternatively, the correlation may be made with the position and size of halogen in appropriate PBHPPs.)

Polymorphism

Polymorphism and thermotropic behaviour is common in polyoxyphosphazenes. For example, solution-grown PB(4-F)PP crystals are monoclinic and have unit-cell dimensions of $a = 2.64$ nm, $b = 1.92$ nm, $c = 0.491$ nm and $\gamma = 86^\circ$ ¹⁷. Such crystals transform into the orthorhombic form when they are heated above $T(1)$ and cooled subsequently to room temperature^{2,16}.

X-ray diffraction patterns of oriented PB(4-H)PP and PB(3-H)PP films are illustrated in Figures 2 and 3. The X-ray diffraction data are listed in Tables 4 and 5. Along with trial unit-cell dimensions are also provided the calculated d -spacings (d_c) and Miller indices. From the X-ray diffraction data for oriented PBHPP specimens, the fibre repeat distances are found to be in the range, $c = 0.480$ – 0.490 nm, which corresponds to the value that has been established for most polyoxyphosphazene

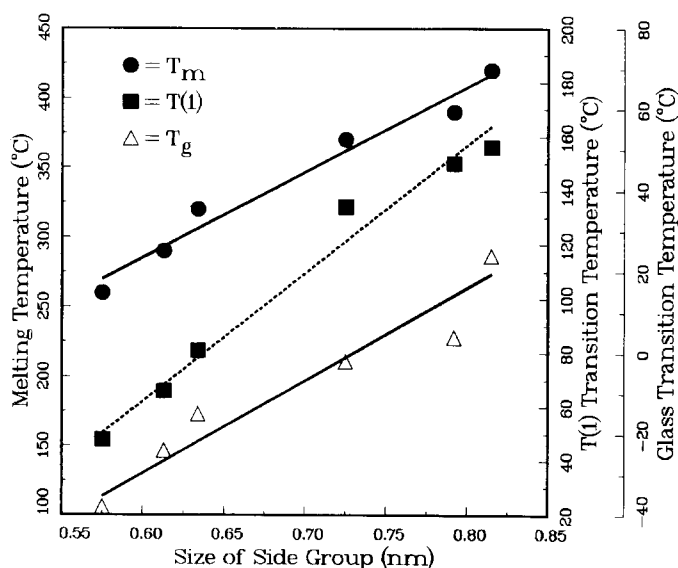


Figure 1 Transition temperatures T_g , $T(1)$ and T_m for PBHPP as a function of side-group size. T_m values are estimated using the empirical equation correlating their parameters

crystals. The calculated X-ray density ρ_c of each polymer was estimated using the appropriate number of monomers (Z) in the unit cell (see Tables 4 and 5), and this is in reasonable agreement with the experimental values (ρ_c) determined by the flotation method. When PB(4-Cl)PP and PB(4-Br)PP crystals are heated through $T(1)$ and cooled, they transform into the orthorhombic (γ -form) structure as found for PB(4-F)PP crystals. The crystal structure of PB(4-Cl)PP crystals has been established by Bishop and Hall⁴ as an orthorhombic unit cell with dimensions $a = 1.308$ nm, $b = 2.023$ nm and $c = 0.490$ nm with space group $P2_12_12_1$. These dimensions are in good agreement with the values found in our work and reported in Table 4* for this polymer after crystals were heated to 200°C (30 min) and then cooled to 25°C . All PB(4-H)PP polymers in Table 4 are orthorhombic. As precipitated, PB(4-Cl)PP and PB(4-Br)PP crystals may be monoclinic (α -form) in line with other polyphosphazenes^{2,8,12} including PB(4-F)PP^{2,16}. PB(3-H)PP crystals exhibit polymorphism; the α - and γ -forms depend upon the treatment temperature. An exception seems to be the α -form of PB(3-Cl)PP, which requires further investigation.

In transformation to the 3D (γ -form) from the 2D thermotropic phase, molecular chains become partially extended and considerable roughening of the crystal surfaces occurs, as has been reported for PBFP²⁵ and PBPP¹⁸. (This change is accompanied by an increase in the polymer crystallinity, which is found to be high when the side-group is small.) Even when PBHPP-type polymers can be crystallized from solution, the crystallinity is comparatively low when the side-groups are large. For PB(4-F)PP, which forms well defined crystals and exhibits distinct electron diffraction patterns^{16,17}, the overall crystallinity is estimated to be below 50%. However, the crystallinity is considerably enhanced whenever materials are heated above $T(1)$ and cooled subsequently to room temperature. PB(4-Br)PP and PB(3-Br)PP, which do not crystallize readily, primarily for steric reasons, are found to be exceptions. The phase change that takes place from the 2D hexagonal phase occurs very slowly, as shown for many polymers

*The a and b axes of PB(4-Cl)PP crystal are switched in Table 4 for convenience of comparison

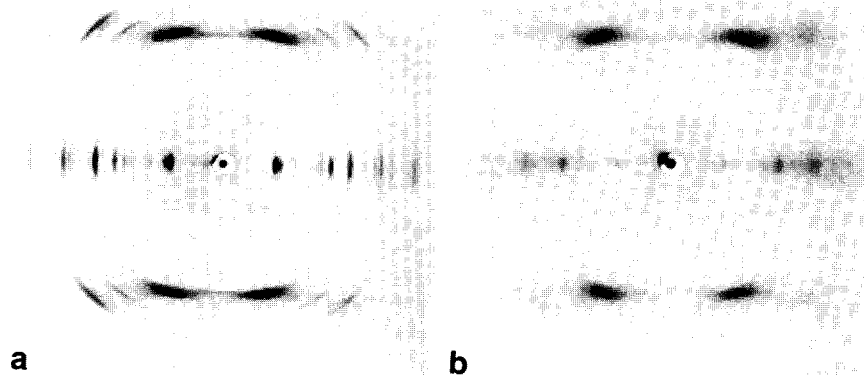


Figure 2 X-ray diffraction patterns of oriented (a) PB(4-Cl)PP and (b) PB(4-Br)PP films. The oriented films were heated to (a) 240°C or (b) 245°C and then cooled to 25°C

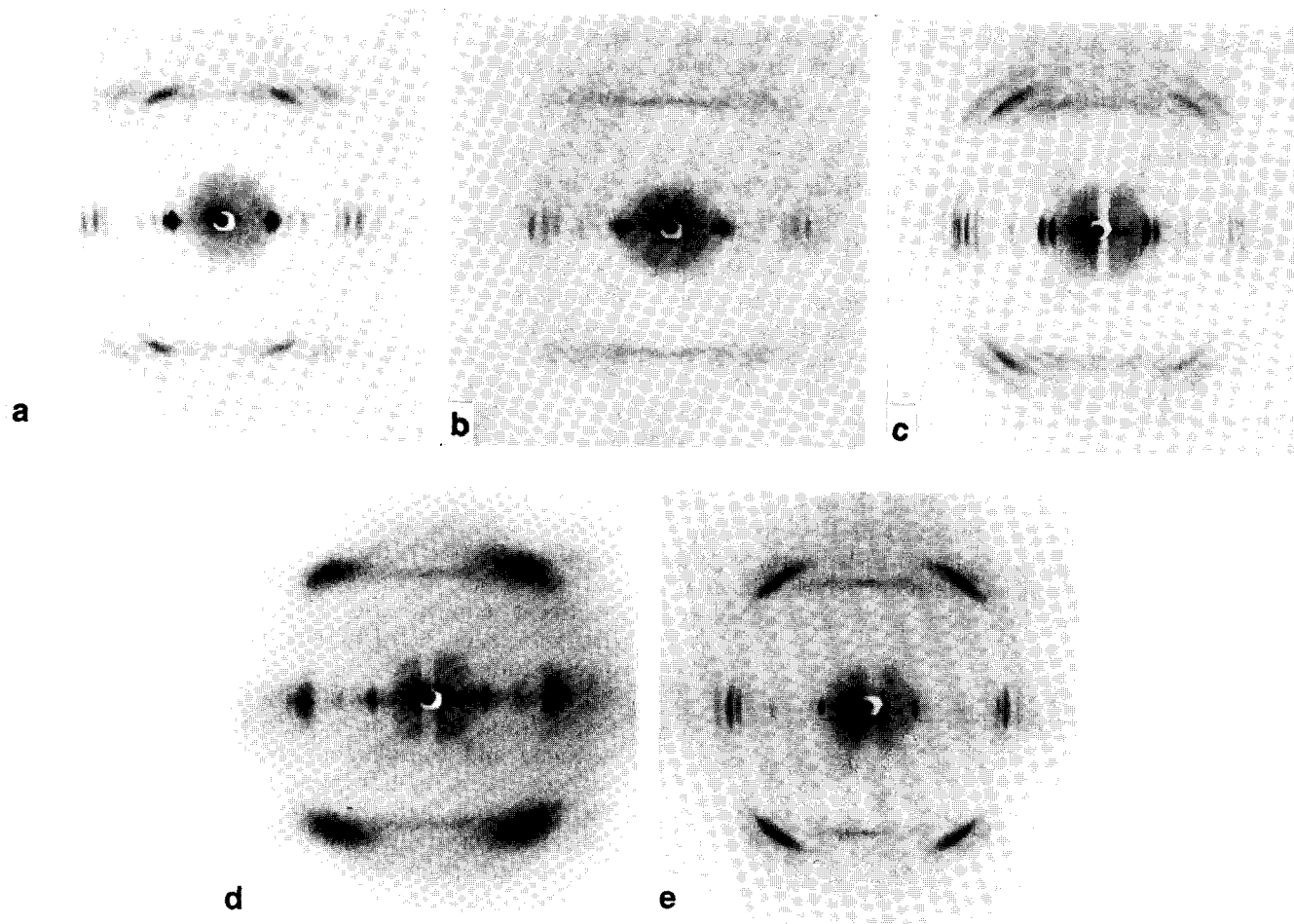


Figure 3 X-ray diffraction patterns of oriented (a), (b) PB(3-F)PP, (c) PB(3-Cl)PP and (d), (e) PB(3-Br)PP films. Patterns for (b), (c) and (e) were obtained for specimens heated above $T(1)$ and cooled to 25°C

that have been monitored by dilatometry²⁷. Table 6 shows density results determined by three different techniques for PBHPP polymers before (I) and after (II) heating specimens above their respective $T(1)$ transitions. Good experimental agreement is obtained with X-ray data for each of the PB(4-H)PP specimens.

Figure 4 represents a series of X-ray diffraction patterns of PB(4-H)PP cast films made under different thermal treatment conditions. For each polymer film cast initially from solution, the crystallinity is found to be relatively low (< 50%). After specimens are heat treated at 200°C and cooled, diffraction patterns taken again at 25°C ((c), (f) and (i)) show well defined 3D scattering patterns in line with a considerably improved crystallinity compared to the original samples. Even PB(4-Br)PP shows some enhancement in crystallinity despite the fact that it may not have crystallized to its fullest extent.

At 200°C ((b), (e) and (h)) diffraction patterns are represented by a diffuse halo and two sharp rings with d -spacings and relative intensities that are listed in Table 7. The ratio of d -spacing values is close to $1:1/\sqrt{3}:1/\sqrt{7}$. These rings correspond to (1 0 0), (1 1 0) and (2 1 0) reflections respectively and are representative of the 2D hexagonal crystal, otherwise designated as the (δ -form). The (1 0 0) reflection depicts the existence of long-range order of a 2D hexagonal conformation having intermolecular distances that increase linearly from 1.32 to 1.45 nm as the size of halogen atom changes from F to Br (Table 7). The intensity of the (1 0 0) reflection

tends to become gradually stronger and sharper, suggesting that the molecular packing is improved after increasing the temperature for PB(4-H)PP specimens that have been subjected to heating and cooling through their respective $T(1)$ transitions. The $\delta \rightarrow \gamma$ transformation for all PBHPP results in a considerable contraction in the plane perpendicular to the molecular chain axis and this is in accord with the high crystallinity that develops. The contraction of 20–30% in the ab plane for PB(4-H)PP-type polymers occurs even though the $T(1)$ transition into the 2D phase for PB(4-Cl)PP involves a 30% expansion in the same plane²⁴. A volume change of $\leq 5\%$ through $T(1)$ has been obtained by dilatometry between 25 and 200°C for PBHPP specimens²⁷. Hence an expansion of more than 10% along the chain molecules would be expected from these polymers. In practice, when the stretched PBHPP films were heated above $T(1)$ and cooled to 25°C as in Figures 2 and 3 for example, an expansion of about 10% was found to occur along the stretched direction. The thermotropic state, because of its expanded nature, has considerable side-group and chain mobility according to recent magic-angle spinning (MAS) n.m.r. results^{23,27}, so that considerable contraction in the ab plane may take place.

Morphology

When polyphosphazene crystals transform from the 2D δ -form to the γ -form or vice versa, a definite

Table 4 Results of X-ray diffraction measurements of poly[bis(*p*-halophenoxy)phosphazenes]^a

PB(4-F)PP heated to 200°C $a = 2.64, b = 1.92, c = 0.485$ nm Orthorhombic (γ) $Z = 8$ $\rho_c = 1.44$ $\rho_o = 1.446$				PB(4-Cl)PP heated to 240°C $a = 2.05, b = 1.31, c = 0.480$ nm Orthorhombic (γ) $Z = 4$ $\rho_c = 1.54$ $\rho_o = 1.481$				PB(4-Br)PP heated to 245°C $a = 2.17, b = 1.29, c = 0.490$ nm Orthorhombic (γ) $Z = 4$ $\rho_c = 1.88$			
(<i>h k l</i>)	d_o	<i>I</i>	d_c	(<i>h k l</i>)	d_o	<i>I</i>	d_c	(<i>h k l</i>)	d_o	<i>I</i>	d_c
(2 0 0)	1.32	m	1.32	(1 1 0)	1.11	vs	1.10	(2 0 0)	1.08	s	1.09
(2 1 0)	1.08	s	1.09	(2 0 0)	1.03	ms	1.03	(0 2 0)	0.645	m(b)	0.645
(1 2 0)	0.901	vw	0.902	(2 1 0)	0.806	m	0.807	(4 0 0)	0.544	s(b)	0.543
(2 2 0)	0.778	m	0.776	(0 2 0)	0.656	m	0.655	(4 1 0)	0.496	vw	0.500
(3 2 0)	0.645	m	0.649	(1 2 0)	0.625	w	0.624	(1 0 1)	0.478	ms	0.478
(3 3 0)	0.519	ms	0.518	(3 1 0)	0.603	m	0.606	(0 3 0)	0.431	vw	0.430
(1 0 1)	0.476	ms	0.477	(2 2 0)	0.551	s	0.552	(4 2 0)	0.416	s(b)	0.415
(5 2 0)	0.465	w	0.463	(3 2 0)	0.473	s	0.473	(1 2 1)	0.381	w(b)	0.384
(6 1 0)	0.429	w	0.429	(1 0 1)	0.469	ms	0.467	(4 3 0)	0.340	m	0.337
(3 0 1)	0.427	s	0.425	(0 1 1)	0.452	s	0.451	(3 2 1)	0.340	m(b)	0.343
(2 2 1)	0.409	w	0.411	(0 3 0)	0.440	vw	0.437	(2 3 1)	0.308	w	0.310
(2 3 1)	0.371	vw	0.371	(2 0 1)	0.436	s	0.435	(3 4 0)	0.294	w	0.295
				(2 3 0)	0.402	m	0.402	(0 1 2)	0.238	w	0.241
				(3 0 1)	0.399	w	0.393				
				(5 1 0)	0.387	ms	0.391				
				(3 1 1)	0.376	ms	0.376				
				(3 3 0)	0.367	m	0.368				
				(4 0 1)	0.349	vw	0.350				
				(5 2 0)	0.345	vw	0.348				
				(4 1 1)	0.337	ms	0.338				
				(6 1 0)	0.329	m	0.331				
				(1 3 1)	0.319	vw	0.319				
				(4 2 1)	0.308	w	0.309				
				(3 4 0)	0.297	w	0.295				

^a(*h k l*) Miller index d_o, d_c Observed and calculated *d*-spacing (nm)*I* Intensity: vs, very strong; ms, medium strong; vw, very weak; etc.; b, broad ρ_c Calculated density from lattice dimensions (g cm^{-3}) ρ_o Observed density by flotation method (g cm^{-3})*Z* Number of monomeric units in the unit cell

relationship exists among the crystallographic axes of the original α -form, the δ -form and the γ -form crystals. A relationship has been established already for PBPP¹². Twinned crystals frequently grow during the $\delta \rightarrow \gamma$ transformation for polyphosphazenes according to an axial relationship^{8,30}. Figures 5a and 5b are electron micrographs of PB(4-F)PP crystals prepared from dilute xylene solution obtained after the sample was heated to 200°C (30 min) and cooled to 25°C on the carbon-coated grids. Figures 5c and 5d are diffraction patterns that were obtained respectively from the original unshadowed and heat-treated PB(4-F)PP crystals. These crystals, originally monoclinic, in agreement with the analysis by Masuko *et al.*¹⁷, were converted into the γ -form (Figure 5d) whenever they passed through the thermotropic phase (δ -form).

Frequently, as thin films, they exhibit a new complicated hexatic morphology as seen in Figure 5b (also see Figure 1a in ref. 16). Hexagonally disposed crystals illustrated in Figure 5b comprise arrays of rod-like crystals; the direction of each rod is parallel to the [a_δ] axis direction of the δ -form, which also

corresponds to the [a_γ] axis direction of the γ -form. This confirmation has been established from electron diffraction measurements (see Figure 5d). The electron diffraction pattern also indicates 60° rotational twinning, as previously reported¹⁶. Thin cast crystalline films of PB(4-F)PP that have been heated above $T(1)$ are illustrated in Figure 6. The morphological features are analogous to the hexatic texture of PBFP films formed when specimens were fused at 250°C ($> T_m$) and then isothermally crystallized at 70°C⁸. Note that this hexagonal morphology has been observed only for a limited number of polyphosphazenes which contain an F atom in the side-group, after heating them above $T(1)$ or T_m and then cooling to room temperature. PBFP crystals do not exhibit this texture unless they were heated above the melting temperature. At this time, we do not understand why the hexatic structure only forms in the PB(4-F)PP films heated in the thermotropic region, and in PBFP films after they have been melted and cooled, but we surmise that the polar side-groups have a 'structuring effect' during crystallization.

Well defined crystals are difficult to form in PBHPP

Table 5 X-ray diffraction results for poly[bis(*m*-halophenoxy)phosphazenes]

PB(3-F)PP heated below $T(1)$ $a = 2.62, b = 2.01, c = 0.485$ nm $\gamma = 86^\circ$ Monoclinic (α) $Z = 8$ $\rho_c = 1.40$ $\rho_o = 1.397$				PB(3-F)PP heated to 175°C $a = 2.57, b = 2.02, c = 0.485$ nm Orthorhombic (γ) $Z = 8$ $\rho_c = 1.41$				PB(3-Cl)PP heated to 165°C $a = 2.38, b = 1.03, c = 0.485$ nm $\gamma = 86^\circ$ $Z = 4$ $\rho_c = 1.68$			
(<i>h k l</i>)	d_o	<i>I</i>	d_c	(<i>h k l</i>)	d_o	<i>I</i>	d_c	(<i>h k l</i>)	d_o	<i>I</i>	d_c
(2 1 0)	1.13	vvs	1.13	(2 0 0)	1.29	vs	1.29	(2 0 0)	1.18	vvs	1.19
(0 2 0)	1.00	m	1.00	(2 1 0)	1.11	vs	1.08	(0 1 0)	1.02	s	1.03
(2 2 0)	0.827	m	0.824	(0 2 0)	1.01	s	1.01	(1 1 0)	0.964	s	0.968
(3 2 0)	0.688	m	0.682	(2 2 0)	0.793	m	0.794	(3 1 0)	0.651	ms	0.649
(0 4 0)	0.502	m	0.501	(4 0 0)	0.640	vw	0.643	($\bar{4}$ 1 0)	0.497	w	0.499
(5 2 0)	0.474	s	0.477	(3 3 0)	0.524	ms	0.529	(2 2 0)	0.483	m	0.484
(0 1 1)	0.471	m	0.471	(0 1 1)	0.474	s	0.472	(1 0 1)	0.476	m	0.475
(6 0 0)	0.435	s	0.436	(2 4 0)	0.469	ms	0.470	(2 0 1)	0.450	w	0.449
($\bar{1}$ 2 1)	0.429	s	0.429	(0 2 1)	0.435	m	0.437	(3 2 0)	0.444	s	0.445
(3 2 1)	0.398	w	0.395	(6 0 0)	0.429	ms	0.428	($\bar{1}$ 1 1)	0.426	m	0.429
($\bar{4}$ 4 0)	0.382	m	0.385	(2 2 1)	0.414	m	0.414	($\bar{3}$ 1 0)	0.420	ms	0.420
($\bar{2}$ 3 1)	0.372	m	0.372	(3 2 1)	0.391	m	0.389	($\bar{3}$ 2 0)	0.416	ms	0.418
($\bar{6}$ 3 0)	0.354	vw	0.354	(2 3 1)	0.372	ms	0.376	($\bar{2}$ 1 1)	0.399	vw	0.407
($\bar{3}$ 3 1)	0.353	w	0.353	(4 2 1)	0.363	m	0.361	(6 0 0)	0.396	m	0.396
($\bar{2}$ 4 1)	0.335	vw	0.333					(3 1 1)	0.384	ms	0.389
(3 6 0)	0.319	w	0.320					($\bar{6}$ 1 0)	0.361	w	0.361
(0 5 1)	0.309	vw	0.309					(4 1 1)	0.359	vw	0.358
(6 6 0)	0.280	w	0.275					(1 2 1)	0.350	s	0.351
								(7 1 0)	0.330	w	0.329
								(5 1 1)	0.326	vw	0.327
								($\bar{7}$ 1 0)	0.317	w	0.316
								(8 0 0)	0.297	w	0.297
								($\bar{6}$ 1 1)	0.288	s	0.290
								(6 3 0)	0.267	vw	0.268
								(3 3 1)	0.267	vw	0.267
								(9 1 0)	0.260	w	0.260
								($\bar{1}$ 4 0)	0.252	ms	0.253
								(1 0 2)	0.240	vw	0.241

Table 6 Density of PB(HP)P polymers

Polymer	Polymer history ^a	Flotation method ^b	Dilatometry	X-ray ^c
PB(4-F)PP	I	1.425	1.42	1.43
	II	1.446	1.45	1.44
PB(4-Cl)PP	I	1.434	1.44	–
	II	1.481	1.48	1.54
PB(4-Br)PP	I	1.753	1.77	–
	II	–	1.77	1.88
PB(3-F)PP	I	1.397	1.41	1.40
	II	–	1.41	1.41
PB(3-Cl)PP	I	1.528	1.47	–
	II	–	1.48	1.68
PB(3-Br)PP	I	1.812	1.85	2.24
	II	–	1.79	2.05

^a(I) Heat-treated below $T(1)$

(II) Heated above $T(1)$ and cooled to room temperature

^bAt 24°C

^cCalculated by unit-cell dimensions in Tables 4 and 5

Table 7 X-ray diffraction results for PB(4-H)PP at 200°C

Polymer	No.	<i>I</i> ^a	<i>d</i> (nm)	(<i>h k l</i>)	a_d (nm) ^b
PB(4-F)PP	1	vs	1.15	(1 0 0)	1.32
	2	w	0.667	(1 1 0)	
	3	b	~0.50	(2 1 0)	
PB(4-Cl)PP	1	s	1.23	(1 0 0)	1.42
	2	vw	0.716	(1 1 0)	
	3	b	0.54	(2 1 0)	
PB(4-Br)PP	1	m	1.26	(1 0 0)	1.45
	2	vw	0.722	(1 1 0)	
	3	b	0.54	(2 1 0)	

^aIntensity: vs, very strong; s, strong; m, medium; w, weak; vw, very weak; b, broad

^bIntermolecular distance in thermotropic phase (at 200°C)

with Cl and Br substituents. For instance, stacks of plate-like crystals of PB(4-Cl)PP precipitated at 135°C from 0.015% w/w xylene solution of polymer are illustrated in Figure 7a. Under the same precipitation

Table 5 continued

PB(3-Br)PP heated below $T(1)$ $a = 2.37, b = 1.00, c = 0.485$ nm $\gamma = 86^\circ$ Monoclinic (α) $Z = 4$ $\rho_c = 2.24$				PB(3-Br)PP heated to 65°C $a = 2.37, b = 1.10, c = 0.485$ nm Orthorhombic (γ) $Z = 4$ $\rho_c = 2.05$ $\rho_o = 1.812$			
($h k l$)	d_o	I	d_c	($h k l$)	d_o	I	d_c
(2 0 0)	1.18	vw	1.18	(2 0 0)	1.18	s	1.19
(0 1 0)	1.00	s(b)	0.998	(1 1 0)	0.996	w	0.998
(3 1 0)	0.642	w	0.641	(4 0 0)	0.594	m	0.593
(1 0 1)	0.477	ms	0.475	(0 2 0)	0.549	w	0.550
(2 2 0)	0.474	s(b)	0.471	(2 2 0)	0.496	w	0.499
($\bar{2}$ 2 0)	0.449	w	0.448	(1 0 1)	0.476	ms	0.475
($\bar{5}$ 1 0)	0.419	w	0.416	(3 2 0)	0.452	ms	0.451
($\bar{2}$ 1 1)	0.402	s(b)	0.405	(2 0 1)	0.450	m	0.449
(4 0 1)	0.373	s(b)	0.375	(1 1 1)	0.434	w	0.436
(0 3 0)	0.333	w	0.333	(5 1 0)	0.432	s	0.435
(3 3 0)	0.316	vw	0.314	(6 0 0)	0.395	m	0.395
(6 0 1)	0.305	w(b)	0.306	(3 1 1)	0.386	s	0.387
($\bar{4}$ 3 0)	0.281	vw	0.282	(1 3 0)	0.363	vw	0.362
($\bar{7}$ 2 0)	0.271	w	0.271	(4 1 1)	0.354	w(b)	0.355
(0 0 2)	0.242	w(b)	0.243	(3 3 0)	0.335	w	0.333
				(3 2 1)	0.331	w	0.330
				(4 2 1)	0.310	vw	0.310
				(7 1 1)	0.269	m	0.269
				(8 2 0)	0.262	m	0.261
				(9 1 0)	0.255	ms	0.256
				(1 0 2)	0.238	w	0.241

conditions, PB(4-Br)PP only forms sheaf-like stacks of crystals, which resemble the spherulitic textures usually encountered in conventional crystalline polymers. Figure 7b is an electron micrograph of the PB(4-Br)PP precipitates. A fracture surface morphology of thicker specimens of PBHPP-type polymers is of particular interest, and the texture depends upon the kind of halogen atom in the phenyl side-group. Scanning electron micrographs of the bulk PB(4-F)PP fracture surface morphology are shown in Figures 8a and 8b. In a parallel investigation micrographs of specimens were made of (i) compressed solution-precipitated polymers (≈ 1 g) normally used for dilatometry²⁷ and (ii) the polymer after heating to 200°C and cooling to 25°C in the dilatometer respectively. Globular materials were found on the surface when PBPP specimens were fractured. This feature is unusual and contrasts with the PBPP specimens, which have shown somewhat complicated fracture surface morphologies that have a rod-like appearance (see Figures 5c and 5d in ref. 18) after specimens have been heated above $T(1)$ (e.g. to 180°C) and cooled. It is conjectured that the long direction of these rod-like moieties corresponds to the chain-extended direction, formed upon crystallization from the 2D to the 3D crystalline phase. Interestingly, the dimensions of the globules on the PB(4-F)PP fracture surface increase in size to $0.15\text{--}0.2\ \mu\text{m}$ after heating to 200°C and cooling to 25°C compared to $0.1\ \mu\text{m}$ diameter in the original specimens. The globular-forming ability in the thicker PBHPP specimens tends to be attenuated accordingly

as the size of halogen atom is increased. The fracture surface of heated PB(4-Br)PP specimens especially forms inhomogeneous globules that differ from those found in PB(4-F)PP. Besides, they are irregularly dispersed in the polymer matrix, as Figure 9 illustrates. In Figure 10, PB(3-Br)PP specimens also show characteristic trends similar to those observed in PB(4-Br)PP. Density measurements (Table 6) made by the flotation method and by dilatometry respectively seem to indicate that a significant increase in crystallinity occurs for heated and subsequently cooled PBHPP specimens. Again PB(4-Br)PP and PB(3-Br)PP are exceptions, because slow crystallization and conformational changes seem to dominate the resultant morphology. The globular textures should be relatable to the crystalline state of the polymer in much the same manner as the rod-like materials in PBPP, which involve extended-chain molecules^{18*}. Fracture seems to occur interglobularly, resembling highly spherically crystallized conventional polymers. The surface and interior morphology of globules has not been determined at this time, but will be the subject of further study.

The globules illustrated in Figure 11a for undrawn PB(4-F)PP film specimens remain partially intact to some degree even after specimens are drawn several times ($\times 5$), followed by heating to 200°C and cooling to 25°C

*There is no evidence, except in *in situ* SAXS measurements, for completely fully extended chains whose identification is extremely difficult in polymers with relative broad *MW* distributions (see Table 1)

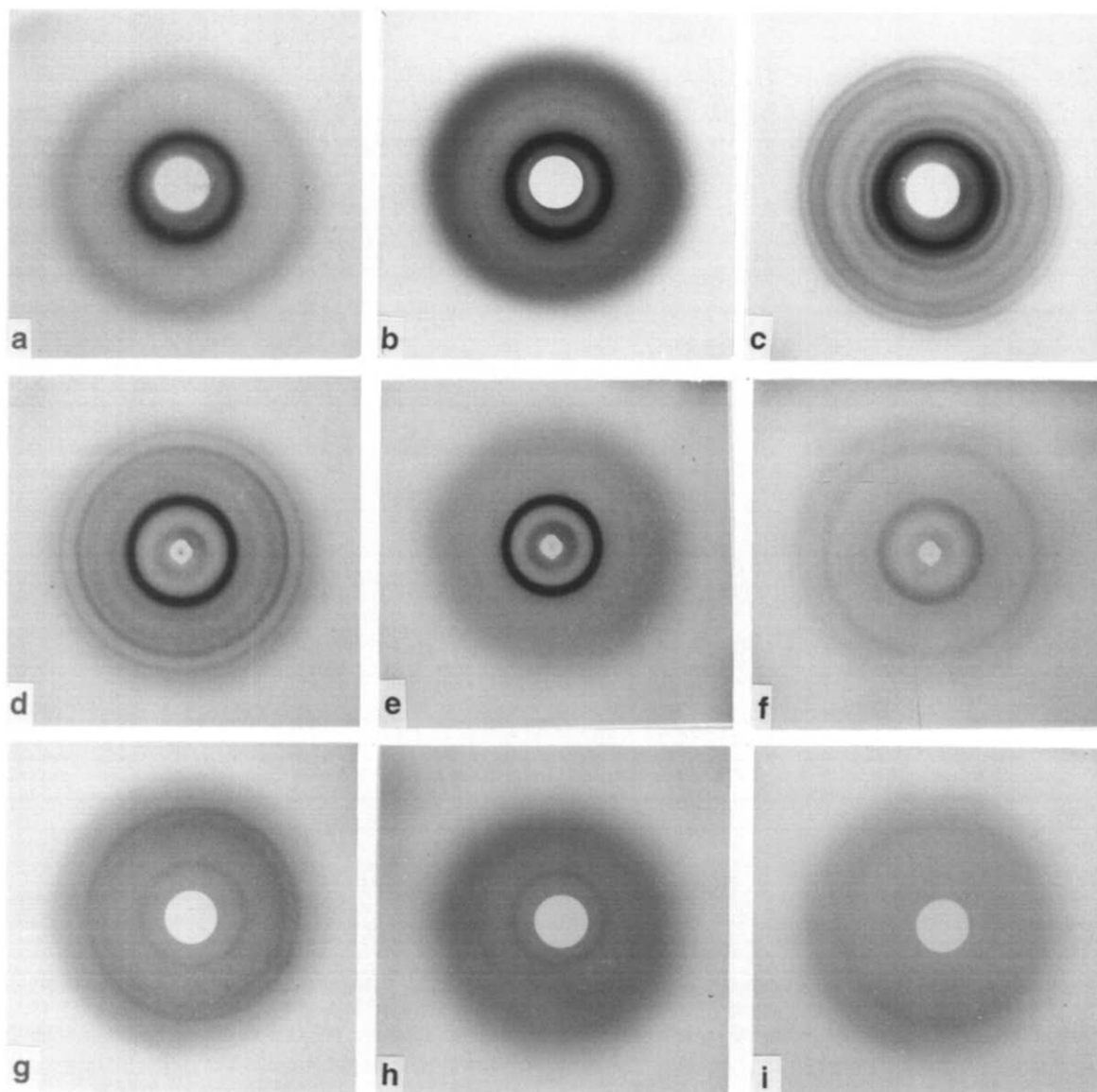


Figure 4 X-ray diffraction patterns of PB(4-HP)P films: (a)–(c) PB(4-F)PP, (d)–(f) PB(4-Cl)PP and (g)–(i) PB(4-Br)PP. The diffraction patterns (a), (d), (g) were taken at 25°C before heating, and (b), (e), (h) at 200°C; also (c), (f), (i) were made at 25°C after heating specimens to 200°C

(see for example the fracture surface in *Figure 11b*). The texture is not fibrillar, as it is in conventional polymer films, but has a granulated necklace-like continuity, which may be 'shish' like. Heat-treated oriented PB(4-Cl)PP and PB(4-Br)PP film specimens indicate fracture surface features that differ from PB(4-F)PP (*Figure 12*). Here, the globules are mostly coalesced and deformed in contact with each other, making a sort of columnar texture. Surprisingly, these deformed globular film specimens exhibit highly oriented X-ray diffraction patterns (*Figure 2*), which are puzzling. The formation of the globules created during solution casting and their growth by later heat treatment of the undrawn films tend to become obscured as group size increases and polarity decreases, on passing from F through Br substituents, a change which is also paralleled by decreasing crystallinity. Undrawn PB(4-F)PP films have the most distinctive globular texture, which becomes obscured on going to drawn PB(4-Cl)PP or PB(4-Br)PP films. Likewise PB(3-Br)PP drawn film specimens exhibit features

displayed in *Figure 13*. The X-ray diffraction patterns of this specimen (*Figure 3e*) are highly oriented even though the specimens comprise globules about 300 nm diameter, and others even less than 100 nm are observed in *Figure 13a*. However, most globules when deformed are oriented in the draw direction as illustrated more clearly in *Figures 13a* and *13b* at higher magnification. In *Figure 13b*, serrated 'edges' are also apparent perpendicular to the draw direction. The spacing of each indentation corresponds roughly to 20 nm, which is of the order of the lamellar thickness in many polymer crystals. A careful inspection of *Figure 13b* suggests a spiral habit, for instance, in the circled region in this micrograph. These deformation features noted in the thicker film specimens are common to all (halophenoxy)phosphazenes whatever their crystallinity, and they depend on the thermal history of the polymer. Basically the globules should comprise highly crystalline materials in line with the X-ray diffraction measurements, but their spherical texture implies that considerable 'space' or openness exists in

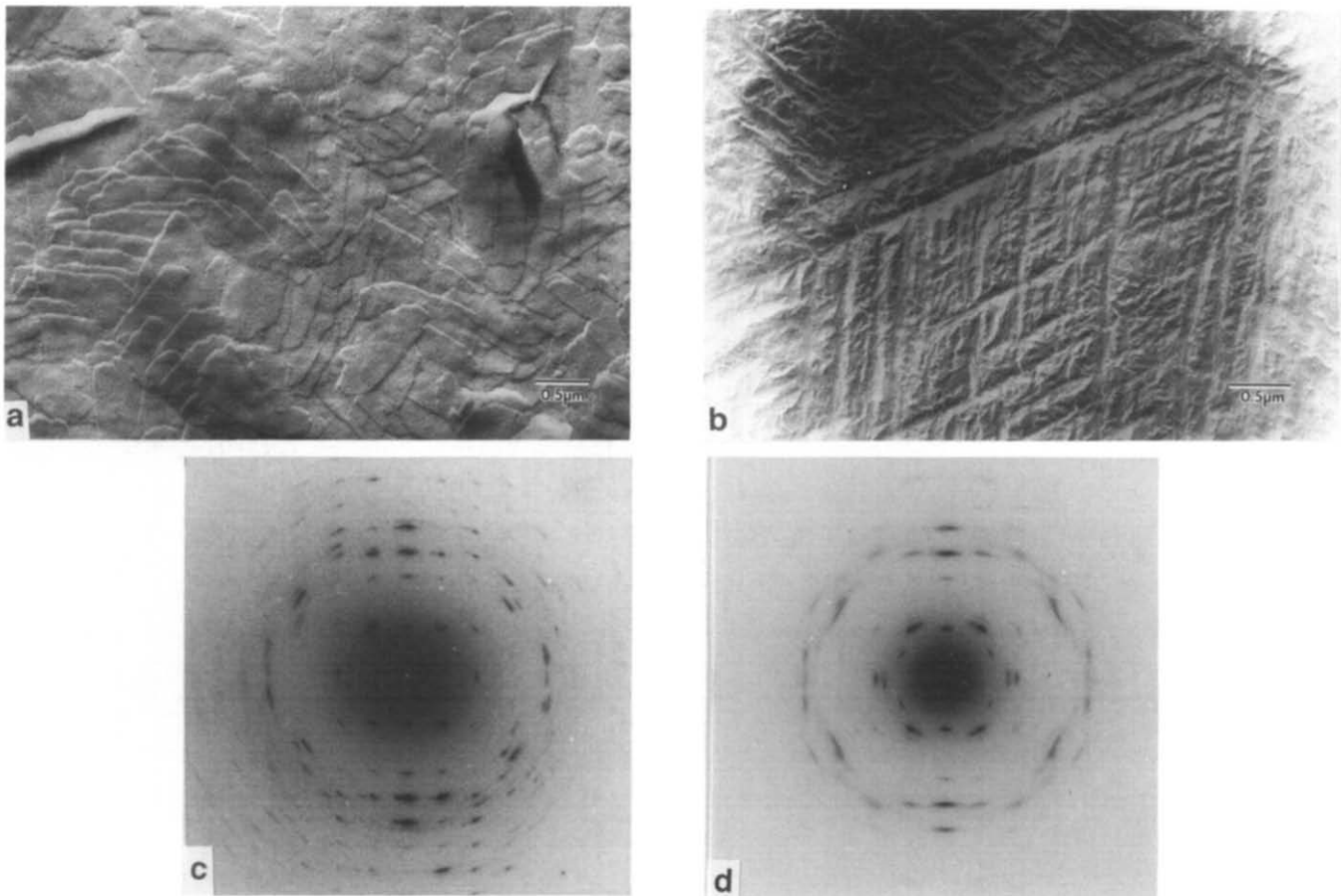


Figure 5 Electron micrographs of PB(4-F)PP crystals prepared from 0.001% w/w xylene solution: (a) as-grown and (b) after heating to 200°C (30 min) and then cooling to 25°C. Electron diffraction patterns were obtained from (c) as-grown crystals and (d) heat-treated crystals

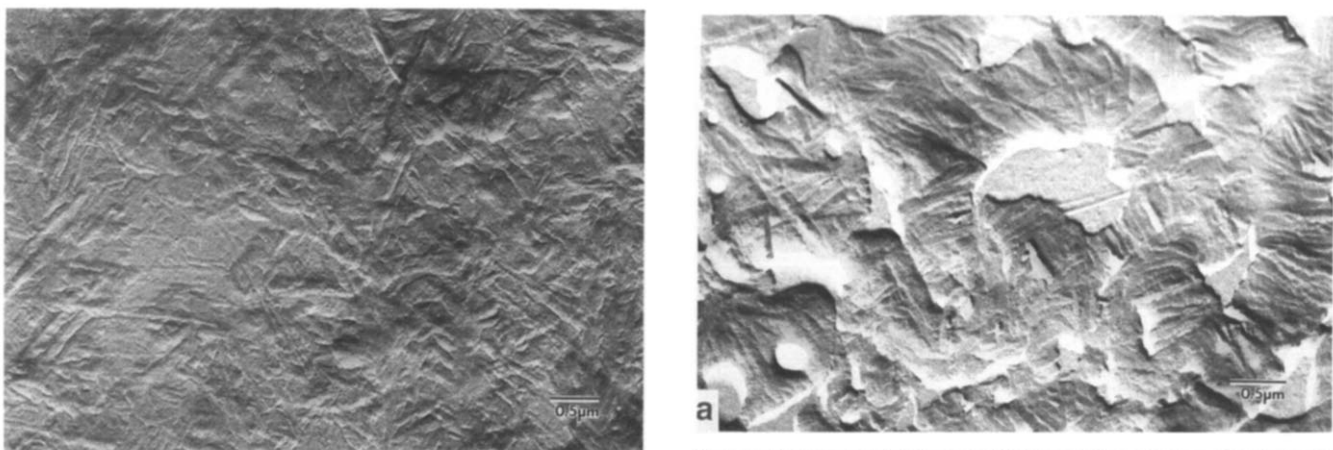
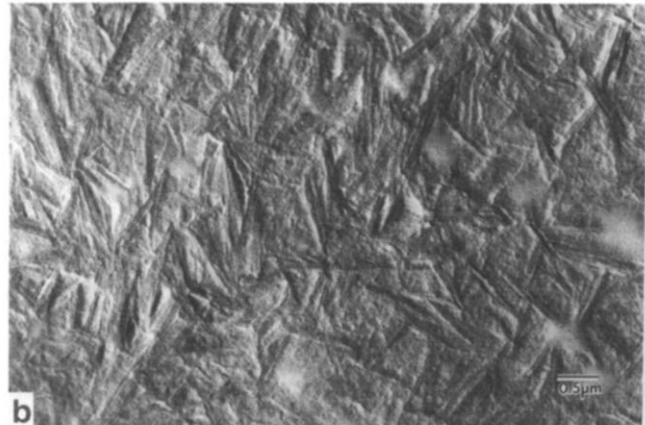


Figure 6 Electron micrograph of THF cast PB(4-F)PP film after heating to 200°C and cooling to 25°C

these specimens, yet the density measurements hardly support the statement! Whenever the specimens are heated the globules grow in size (a kind of Ostwald ripening† occurs) if they have an irregular shape (e.g. Figure 8). Chain-extended crystals have already been documented for some polyphosphazenes after they are

† In a sense equivalent to a hierarchial or supramolecular texture, which is not foreign to mesophases

Figure 7 Electron micrographs of (a) PB(4-Cl)PP and (b) PB(4-Br)PP thin films cast from 0.015% w/w xylene solution at 135°C



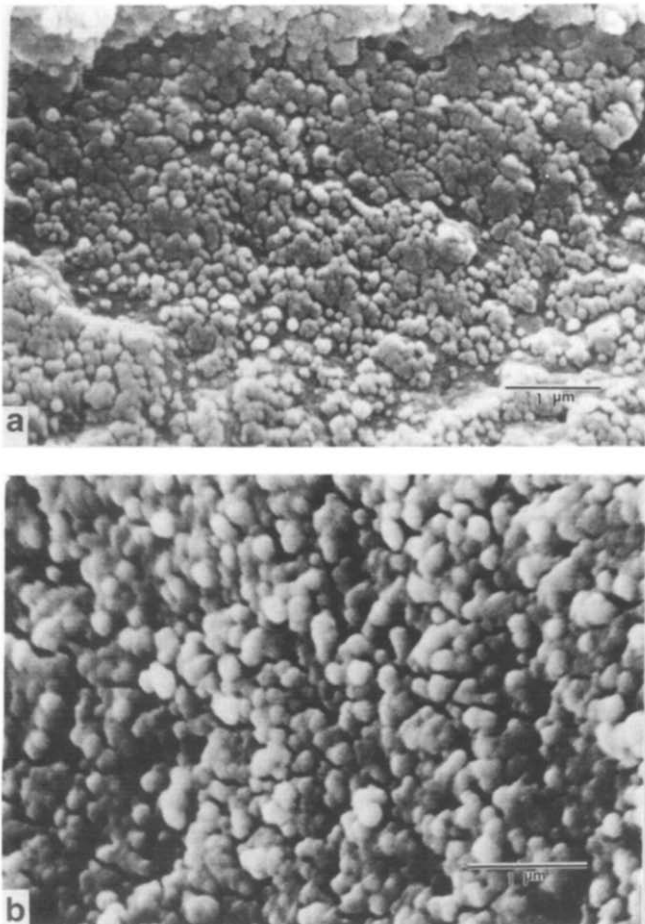


Figure 8 Fracture surface morphology of PB(4-F)PP disc specimens used for dilatometry: (a) initially compressed, (b) after heating to 200°C and cooling to 25°C in the dilatometer

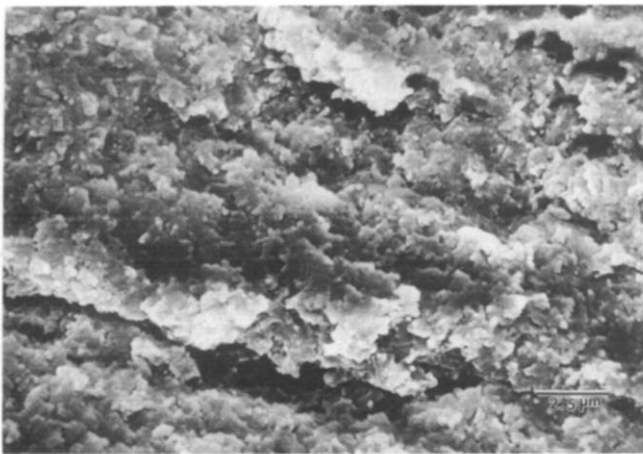


Figure 9 Fracture surface morphology of PB(4-Br)PP cast film after heating to 200°C, followed by cooling to 25°C

crystallized through the $T(1)$ transition³¹. There seems to be a common feature in PBHPP materials where an increase in size of the globules occurs upon heat treatment, with a tendency to become irregular in shape. These are still puzzling features. For example, the specimens have porous features from the viewpoint of the fracture surface morphology, yet specimens after heat treatment and crystallization have a high density, almost approaching the crystallographic unit-cell values in some examples. These problems will be tackled in further ongoing investigations.

CONCLUSIONS

Poly[bis(halophenoxy)phosphazenes] with F, Cl and Br in the *para*- or *meta*-phenoxy substituents were synthesized for structural and morphological investigations.

The transition temperatures T_g and $T(1)$ for each polymer roughly show a linear increase with the size of halogen atom. Chain stiffness and segmental immobility is reflected in an increase in T_g , which is in the line with anticipated trends in properties.

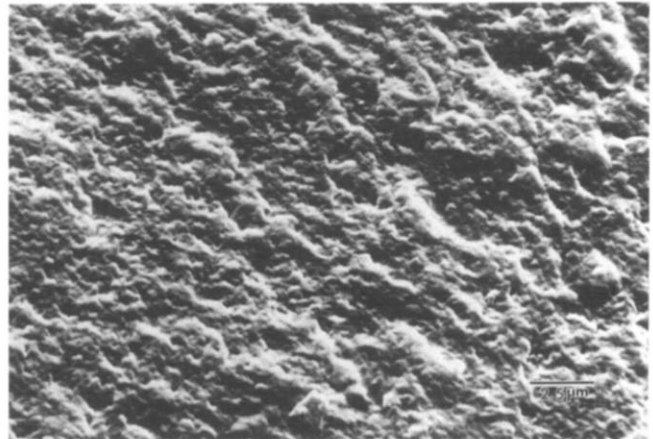


Figure 10 Fracture surface morphology of PB(3-Br)PP disc specimen after heating to 200°C, followed by cooling to 25°C in the dilatometer

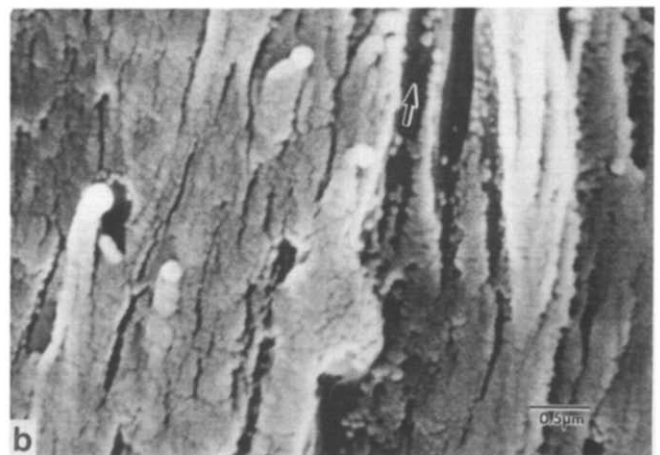
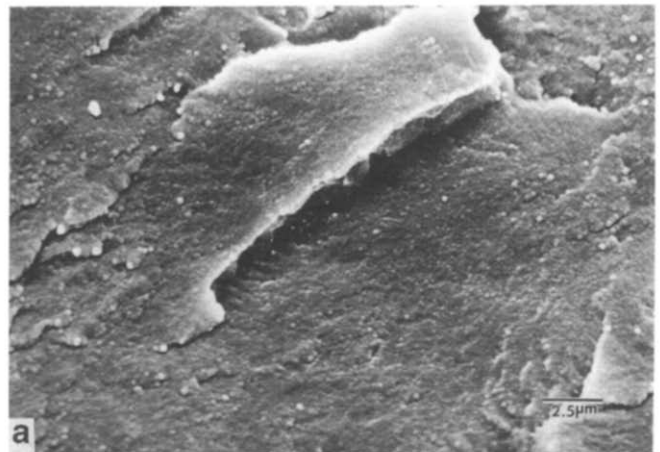


Figure 11 Fracture surface morphology of PB(4-F)PP thicker film specimens: (a) as cast, (b) heated to 200°C after drawing five times, at or below $T(1)$. The arrow indicates the draw direction

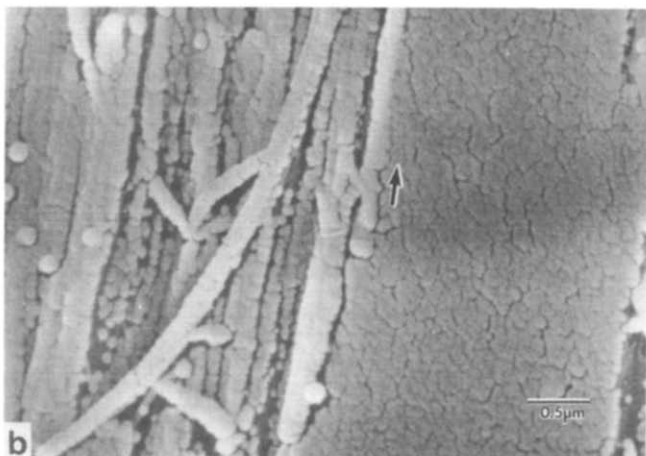
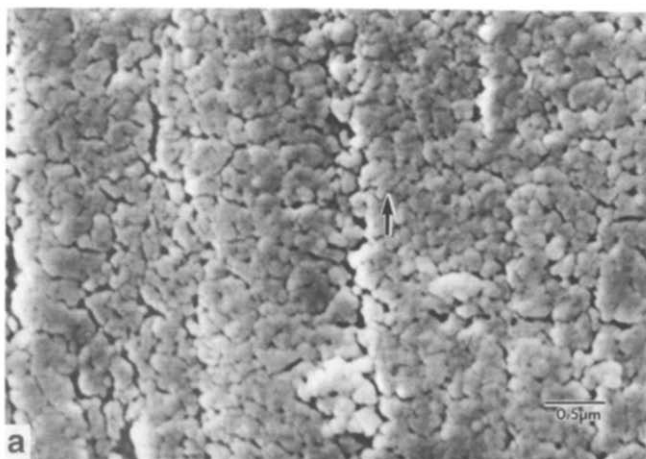


Figure 12 Fracture surface morphology of oriented films: (a) PB(4-Cl)PP films (heated to 240°C), (b) PB(4-Br)PP films (heated to 245°C). The arrow indicates the draw direction

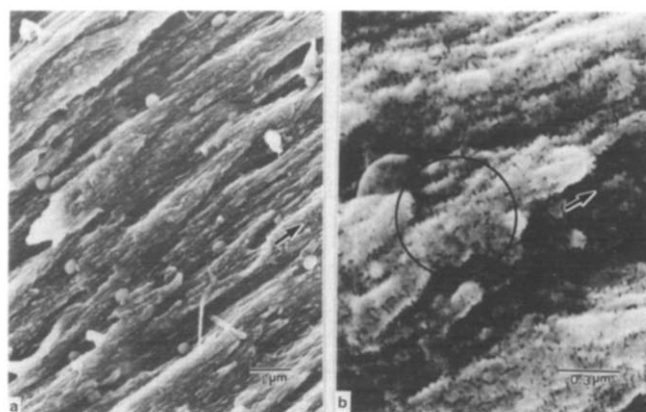


Figure 13 Fracture surface morphology of PB(3-Br)PP films: (a) low magnification. (b) higher magnification. The arrow indicates the draw direction. The specimens were coated with Au

The structure of solution-cast halophenoxyphosphazenes is monoclinic and this transforms to the orthorhombic (γ) form after heating above and cooling down through the $T(1)$ transition. Above $T(1)$ the structure is pseudohexagonal.

The transformation through $T(1)$ for PBHPP results in a surprising contraction (or expansion) of 20–30% in the crystallographic ab plane with an expansion (or contraction) of more than 10% along the chain molecule direction.

The intermolecular distances in thermotropic phases increase linearly on increasing the side-group dimensions.

Generally, the ability of the polymers to crystallize decreases and the ease of formation of well defined crystals decreases as the size of halogenated phenoxy increases and the polarity of the halogen decreases.

PB(4-F)PP crystals often form a hexatic morphology upon cooling through $T(1)$ from the thermotropic phase.

PBHPP thicker specimens form globules, which grow into irregular shapes and become less distinct as the halogen size changes from F to Br.

Fracture surfaces of the highly oriented PBHPP film specimens show bundle-like textures that comprise irregularly shaped globules. The bases for their formation is unknown.

ACKNOWLEDGEMENTS

The authors are grateful to the National Science Foundation (Polymer Program) and to Chisso Corporation for partial support of this work.

REFERENCES

- 1 Sokolskaya, I. B., Freidzon, Ta. S., Kochervinski, V. V. and Shibayev, V. P. *Polym. Sci. USSR* 1986, **28**, 329
- 2 Kojima, M. and Magill, J. H. *Polymer* 1989, **30**, 579
- 3 Beres, J. J., Schneider, N. S., Desper, C. R. and Singler, R. E. *Macromolecules* 1979, **12**, 566
- 4 Bishop, S. M. and Hall, I. H. *Br. Polym. J.* 1974, **6**, 193
- 5 Allcock, H. R. and Arcus, R. A. *Macromolecules* 1979, **12**, 1139
- 6 Allcock, H. R., Arcus, R. A. and Stroh, E. G. *Macromolecules* 1980, **13**, 919
- 7 Burkhart, C. W., Gillete, P. C. and Lando, J. B. *J. Polym. Sci., Polym. Phys. Edn* 1983, **21**, 2349
- 8 Kojima, M. and Magill, J. H. 'Morphology of Polymers' (Ed. B. Sedlacek), Walter de Gruyter, Berlin, 1986, p. 435
- 9 Magill, J. H. and Rieckel, C. *Makromol. Chem., Rapid Commun.* 1986, **7**, 287
- 10 Meille, S. V., Porzio, W., Allegra, G., Audisio, G. and Gleria, M. *Makromol. Chem., Rapid Commun.* 1986, **7**, 217
- 11 Magill, J. H., Petermann, J. and Rieck, U. *Colloid Polym. Sci.* 1986, **264**, 570
- 12 Kojima, M., Satake, H., Masuko, T. and Magill, J. H. *J. Mater. Sci. Lett.* 1987, **6**, 776
- 13 Meille, S. V., Porzio, W., Bolognesi, A. and Gleria, M. *Makromol. Chem., Rapid Commun.* 1987, **8**, 43
- 14 Chatani, Y. and Yatsuyanagi, K. *Macromolecules* 1987, **20**, 1042
- 15 Chatani, Y. *Polym. Prepr. Japan* 1989, **38**, 4339
- 16 Kojima, M., Masuko, T. and Magill, J. H. *Makromol. Chem., Rapid Commun.* 1988, **9**, 565
- 17 Masuko, T., Hoshi, M., Kitami, J. and Yonetake, K. *J. Mater. Sci. Lett.* 1988, **7**, 1241
- 18 Kojima, M., Sun, D. C. and Magill, J. H. *Makromol. Chem.* 1989, **190**, 1047
- 19 Kojima, M. and Magill, J. H. *Polymer* 1989, **30**, 1856
- 20 Kojima, M. and Magill, J. H. *Makromol. Chem.* submitted
- 21 Cypryk, M., Matyjaszewski, K., Kojima, M. and Magill, J. H. *Makromol. Chem., Rapid Commun.* 1992, **13**, 29
- 22 Allen, G., Lewis, C. J. and Todd, S. M. *Polymer* 1976, **11**, 44
- 23 Young, S. G. and Magill, J. H. *Macromolecules* 1989, **22**, 2549
- 24 Desper, C. R. and Schneider, N. S. *Macromolecules* 1976, **9**, 424
- 25 Kojima, M., Kluge, W. and Magill, J. H. *Macromolecules* 1984, **17**, 1421
- 26 Mujumdar, A. N., Young, S. G., Merker, R. L. and Magill, J. H. *Macromolecules* 1990, **23**, 14
- 27 Young, S. G. Ph.D. Thesis, University of Pittsburgh, 1990; Young, S. G., Kojima, M. and Magill, J. H. *Polymer* in press
- 28 Sun, D. C. and Magill, J. H. *Polymer* 1987, **28**, 1243
- 29 Young, S. G., Kojima, M. and Magill, J. H. ACS Meeting, Miami, 10–15 September, 1989
- 30 Kojima, M. and Magill, J. H. *Polym. Commun.* 1988, **29**, 167
- 31 Kojima, M. and Magill, J. H. *Polymer* 1985, **26**, 1971
- 32 Magill, J. H. *J. Inorg. Organomet. Polym.* 1992, **2**, 213